ResearchGate

See discussions, stats, and author profiles for this publication at: https://www.researchgate.net/publication/233811084

Shipra G, Gauri M, Chandra PM, Kishore SP (2012) Identification of novel potent inhibitors against Bcl-xL anti-apoptotic protein using docking studies.Protein Pept Lett. 9. PMID: 2...

Article *in* Protein and Peptide Letters · June 2012

DOI: 10.2174/092986612803521602

CITATIONS
10

READS
142

4 authors, including:

Shipra Gupta
GVK Bio
18 PUBLICATIONS **154** CITATIONS
SEE PROFILE

Gauri Misra
National Institute of Biologicals
38 PUBLICATIONS **245** CITATIONS
SEE PROFILE

Prahlad Seth
Biotech Park Lucknow
355 PUBLICATIONS **7,661** CITATIONS
SEE PROFILE

Some of the authors of this publication are also working on these related projects:

Human resource management View project

in Silio Search for Biomerkrs for neurological disorders View project

All content following this page was uploaded by Shipra Gupta on 23 December 2013.

The user has requested enhancement of the downloaded file.

Identification of Novel Potent Inhibitors Against Bcl-xL Anti-apoptotic Protein Using Docking Studies

Gupta Shipra*[,1,#], Misra Gauri[2,#], Pant Mohan Chandra[3] and Seth Prahlad Kishore[1]

[1]*Biotech Park, Sector-G Jankipuram, Lucknow-226021, Uttar Pradesh, India;* [2]*Hygia Institute of Pharmaceutical Education and Research, Lucknow, Uttar Pradesh, India;* [3]*Department of Radiotherapy, C. S. M. Medical University, Shahmina Road, Lucknow-226003, Uttar Pradesh, India*

Abstract: Bcl-xL protein belongs to BCL-2 family which has either pro- or anti-apoptotic activities owing to their importance in the regulation of apoptosis, tumor genesis and cellular responses to anti-cancer therapy. Bcl-xL permeabilize the outer mitochondrial membrane of cells and inhibit these processes. Protein–inhibitor interactions play an important role in regulating the expression of Bcl-xL protein. Here, we report the docking studies that resulted in the identification of new inhibitors distinct from the previously reported inhibitor against this protein. The results have been validated using Sybyl surflux docking. New potent inhibitors from docking analysis are pentacyclic triterpenoid derivative (2S,4aR,6aR, 6bS,8aS,10R,12R,12aS,12bR,14bR,E)-10,12-dihydroxy-2,4a,14b-trimethyl-9-((((R)-3,4,5-trihydroxy-6-methyl-2H-pyran-2-yl)oxy)methylene)-1,2,3,4,4a,5,6,6a,6b,8a,9,10,11,12,12a,12b,13,14b-octadecahydropicene-2-car-boxylic acid and 4-alkyl-4-methoxypiperidine derivative 8h (where R= 4-Cl-Ph) that promotes the release of pro-apoptotic proteins from the mitochondria which is a key event in cell death signaling. The compounds form stable complex with protein exhibiting highest binding affinity and Gibbs free energy. Pentacyclic triterpenoid derivatives compound-201 and piperidine derivative compound-39 are potent inhibitors with Ki value of 172.62nM and 175.24 nM high affinity and inhibitory potency. Salt bridge, pi-pi and hydrogen bonding interactions predominantly contribute towards the stability of the complexes. These compounds can further be exploited for their potential to enhance apoptosis. We have established the correlation between the experimental Ki value with our computational inhibition constant. The quantitative predictions in this study provide a scope for further experimental testing giving structural insights into the design and development of novel anti-cancer drugs.

Keywords: Bcl-xL protein, chemical fingerprint, apoptosis, molecular docking, molecular interactions.

INTRODUCTION

Trial-and-error tests using cell and animal model are established techniques for conventional drug designing. Specialized labs requiring high-throughput screening for chemicals with desired bio-activities make the conventional process tedious and expensive. With increasing number of known experimental target molecules, computational methods have been used to significantly supplement and expedite the drug designing process. In silico drug designing involves various methods of virtual screening, pharmacokinetics, chemoinformatics and interaction analysis. This multi-disciplinary field has accelerated the drug research by determining the potential therapeutic effectiveness of designed target molecules prior to laborious experiments and expensive preclinical trials. In silico analysis is the most straight forward approach to discover and predict novel lead molecules. In the present study we have used chemoinformatics and computational design techniques to identify small molecules that could potentially promote cancer cells death by inhibiting Bcl-xL protein.

*Address correspondence to this author at the Bioinformatics Centre, Biotech Park, Sector-G Jankipuram, Lucknow-226021, Uttar Pradesh, India. Tel: +91(522)4053010; Fax: +91(522)4012081;
E-mail: shiprabioinfo@gmail.com
# Both the authors are first author and has equal contribution in the manuscript.

Apoptosis (programmed cell death) is highly conserved and regulated process, which is the primary mechanism for the removal of aged, damaged, and unnecessary cells. Its deregulation can lead to severe human diseases like neurodegenerative disorders, viral infections, cancer development and poor response to conventional chemotherapy [1]. Cellular proteins of Bcl-2 family are crucial and fundamental component of apoptosis and include members that either prevent (e.g. Bcl-2 or Bcl-xL) or promote (e.g. Bax or Bak) the membrane permeabilization [2]. The up-regulation of Bcl-2 or Bcl-xL anti-apoptotic protein in cancer such as head and neck squamous cell carcinoma (HNSCC) is linked to aggressive tumor growth, metastasis and chemo-resistance [3]. More than 500,000 new cases of HNSCC are detected every year and it is one of the leading causes of cancer related deaths, worldwide. The tumor has been caused by the deregulation of apoptosis and mediates resistance to cancer therapy [3].

Furthermore, thorough understanding of Bcl-xL—inhibitors binding at interaction level introduces a novel marker for anticancer drug design. Malignant cells can evade death signals by over expressing anti-apoptotic proteins, inhibiting proapoptotic activators, or precluding BAX and BAK activation. Together all these can lead to reduced chemotherapy response. Disabling of antiapoptotic proteins is often desired for the advancement of apoptosis [4]. Thus,

0929-8665/12 $58.00+.00 © 2012 Bentham Science Publishers

generation of small molecule inhibitors to Bcl-xL can sensitize HNSCC cells for chemotherapeutic agents [3].

Three dimensional structural studies of anti-apoptotic Bcl-2 family proteins provide insight about the protein interaction to pro-death counterparts. The hydrophobic region of the protein is known to be a membrane anchor domain and it is involved in inhibitor recognition. The A chain comprises of 7-8 alpha helixes and the pro-survival protein has four conserved hydrophobic residues (h1–h4) on one face of a helix that inserts into hydrophobic pocket (p1–p4) within the hydrophobic groove [5]. These hydrophobic amino acids are important in membrane docking resulting in permeabilization [6]. The reported small molecule biarylacylsulfonamide allows BAX and BAK activation by binding Bcl-xL protein and disrupting their complexes with proapoptotic proteins. Various studies revealed that biarylacylsulfonamide was lethal to many cancer cells. Therefore, it has biarylacylsulfonamide emerged as an efficient agent against human follicular lymphoma cell lines that over express Bcl-xL [7].

In the present study, we propose the binding activity of Bcl-xL protein involved in inhibition of apoptosis with the screened inhibitors. The compounds are screened on the basis of their similarity with the biarylacylsulfonamide derivative (where R=2-biphenyl) and adjudged by their efficacy and sensitivity. These compounds majorly comprise of piperidine and polyphenol scaffold. The discovery of these potential inhibitors against Bcl-xL opens new avenues for designing compounds that could target the interaction of Bcl-xL with Bax — an important protein that directly activates the apoptosis. This is the first report to the best of our knowledge that explores the fingerprinting against Bcl-xL. Bcl-xL represents an attractive target for novel anti-cancer agents designed to overcome chemotherapy resistance in cancer cells.

MATERIAL AND METHODS

Selection and Preparation of Macromolecule

Crystal Structure of the Bcl-xL protein (PDB id: 2YXJ) was retrieved from PDB databank (http://www.pdb.org/) [6, 8]. The protein as well as inhibitors optimization was carried out using sybyl-x1.1 utilizing conjugate gradient method (TRIPOS Inc. 1699, South Hanley Road, St. Louis, Mo 63144, USA). The binding pocket of the protein was determined by grid based approach using default parameters and resolution of 0.5 Å [9]. Rigid docking was performed for studying protein-inhibitor interactions through Auto Dock Tools. The atom types and bond types were assigned and only polar hydrogens were added to neutralize the protein [10, 11]. The grid maps were generated using docking grids of 60*60*60 points spanning binding pocket of the protein with the grid point spacing of 0.431 Å. The grid map covered the active site along with the significant portions of the surrounding surface [9].

Virtual screening and Chemical Fingerprinting of inhibitors dataset

The 427 analogs of the inhibitor were screened from binding database (http://www.bindingdb.org). Drugs were screened based on the pharmacological properties (IC50 and Ki values). To calculate the similarity between analogs, their fingerprints were generated by Smart Pattern FF3 method using Open Babel software (http://openbabel.org). The qualitative and quantitative characterization such as physiochemical properties was done using molinspiration web server (http://www.molinspiration.com) as summarized in Table **S1**, **S2**. Tanimoto coefficient of fingerprints was used to determine the chemical and topological features of small molecules as shown in the Table **1**. Drug optimization was carried out using sybyl-x1.1 with conjugate gradient method (TRIPOS Inc. 1699, South Hanley Road, St. Louis, Mo 63144, USA).

Molecular Docking and their Interaction Studies

Molecular Docking of screened compounds (Tanimoto coefficients is in range of 0.9 to 1.0) was carried out using Lamarckian genetic algorithm inbuilt in Autodock4.2 tools with default docking parameters. We selected Autodock4.2 tool for the purpose of molecular docking because it has been established as a method that consistently yield enrichments in comparison to other methods with higher accuracy and certainty [12]. The macromolecule was prepared to calculate the binding energy. The polar hydrogens were added whereas the non-polar hydrogens were removed from the protein coordinates and the Gasteiger partial charges were further added to the carbon that held the hydrogen. The atom type for the aromatic carbons was reassigned to be handled by the aromatic carbon grid map. Grid parameter files were built and atom-specific 3D affinity maps were constructed using Autogrid4. The three docking steps (van der Waals interactions, hydrogen bonds and the electrostatic potential) were considered for the calculation of binding energy. The relationship between the protein and the ligand was described by Lamarckian genetic algorithm through orientation, conformation and translation of the ligand. Each docking experiment was derived from 10 different runs that were set to terminate after a maximum of 2,500,000 energy evaluations or 27,000 generations, yielding 10 docked conformations and the population size was set to 150. The elitism number, the rate of gene mutation and the rate of gene crossover were 1, 0.02 and 0.8 respectively. After generation of multiple runs, cluster analysis was performed. The docking solutions with inhibitors having all atom RMSDs within 2.0 Å of each other were clustered together and ranked by their lowest energy, respectively. The lowest-energy solution was accepted as the best docking conformation for the binding energy calculation. However, after each docking calculation, the RMSD between the lowest energy docked ligand pose and the complex crystal structure ligand pose was evaluated. Docking interactions were clustered to determine free energy of binding and optimal docking energy conformation was considered as the best docked pose [9, 13]. Subsequently, the RMSD was calculated using optimal energy ligand conformation obtained after each run. RMSD calculations were performed using protein–compound-201, exhibiting lowest inhibitory constant as the template using Accelrys Discovery Studio Visualizer2.5 (Discovery Studio, Version 2.5; Accelrys, Inc. San Diego, CA, USA, 2009).

Alternatively, docking was carried out between compounds and protein to check the variation in the existing interactions in the binding pocket ranging from 0.1-0.2 with

the previously known interactions (Tanimoto coefficients 0.9-1.0) in the binding pocket. The generated conformations had an associated value of binding free energy. An estimated inhibition concentration (Ki) was used for determination of binding energies of different docking conformations, ranking in accordance to their binding scores [14]. For the estimation of binding free energy in kcal/mol the electrostatic energy, van der Waals, hydrogen bond, desolvation energy, total intermolecular and torsional energy of binding were used and Gibbs free energy of binding was calculated (Table **2** and **3**) [14-17]. A 2 Å RMSD constraint with respect to the 2YXJ crystal structure was set for studying protein-inhibitor interactions. All the docking experiments were done under physiological pH of the protein and compounds. New external charges have been added during the procedure.

RESULTS

Rationale for Macromolecule and Ligands Selection

The dataset of 427 inhibitors against Bcl-xL protein was used to determine the inhibition efficacy of various compounds against the protein that prove to be more potent than the reported inhibitor [18-20] for the apoptosis of head and neck squamous cell carcinoma [21].

Virtual Screening and Chemical Fingerprinting of Inhibitors Dataset

Chemical fingerprinting was applied to range the number of inhibitors from lowest to highest similarity, which were further used for docking as summarized in Table **1**. As a result, 50 compounds were detected that exhibited close similarity to the reference compound i.e. a potent biarylacylsulfonamide antagonists (i.e. R= 2-biphenyl) of the antiapoptotic protein Bcl-xL [20]. Tanimoto coefficients for these compounds was in the range of 0.9 to 1.0 where as 49 compounds were screened with more divergence and Tanimoto coefficients ranging from 0.1 to 0.2 (structures shown in Fig. (**1**)(**A**, **B**, **C** high similarity and **D**, **E**, **F** low similarity)) [22]. Pharmacological properties and physiochemical properties of the compounds are summarized in Table **S1** and **S2**.

Docking Studies and Energy Calculations

The 51 highly similar and 49 dissimilar inhibitors that were screened based on various parameters described earlier were docked to Bcl-xL protein using Lamarckian genetic algorithm. Phe97, Arg100, Tyr101, Arg102, Arg103, Phe105, Asp107, Leu108, Gln111, Glu129, Leu130, Asn136, Gly138, Arg139 and Ala142 are the predominant residues lining the binding pocket. The docking results, the predicted binding energies and inhibitory constants were calculated for all of them (Table **2**, **3**). The results of predicted binding energies were clustered to determine the optimal docking energy conformation that is considered as the best interacting pose for both low similarity compounds and the most similar compounds. Further, the results were confirmed using different grid size spanning different regions of the protein. Unanimously both types of compounds had indicated that the Bcl-xL interaction with inhibitors decrease the anti-apoptotic activity for the protein. However, the most potent dissimilar compound showed better interactions and docking score than the similar ones.

Table 1. Drug Selection Criteria through Chemical Finger Printing

Range of Tanimoto Coefficient	No. of Compounds
0.0-0.1	2
0.1-0.2	49
0.2-0.3	193
0.3-0.4	29
0.4-0.5	4
0.6-0.7	6
0.7-0.8	26
0.8-0.9	67
0.9-1.0	51

Protein–ligand Interactions

Based on the energy values and binding interactions for various protein-inhibitor complexes, three out of the forty nine lowest similarity group and twelve out of fifty inhibitors constituting the highest similarity group, two inhibitors from each group were selected as the best inhibitors based on the optimal binding energy. Compound-39 and compound-201 has the optimal docking energy and exhibit best docking interactions with the protein.

In the highest similarity group, compound-4 has the optimal docking energy but it forms only two hydrogen bonds with Tyr101 and Ala142 residues. On the other hand, compound-5 and compound-37 forms only one hydrogen bond with Arg139 and Asn136 residues of the binding pocket. Compound-2 and compund-11 were screened out as they do not show any interaction with the protein, despite their low docking energies. The binding pocket shows salt bridges that contribute towards the stability of the binding pocket. Similarly, compound-6, compound-13, 18, 41 and 56 are good inhibitors but the docking energy and the interactions with protein are poor in comparison to compound-39. These compounds show only one hydrogen bond where as compound-11 exhibits only one pi- interaction. They show weaker interactions than the compound-39. Compound-12 forms one hydrogen bond, one pi-interaction with Glu129 and Tyr101 residues of the binding pocket. Compound-37 and compound-5 forms only one hydrogen bond and two pi interaction with Tyr101, Asn136, Arg139, Tyr195 and it also forms salt bridge with Glu96:Arg100 contributing towards the stability of the binding pocket. Despite optimal docking score, compound-39 forms one salt bridge with Asp107:Arg103, one pi-pi interaction with Tyr101 and two hydrogen bonds with Arg39, Ala142 that are hydrophobic in nature, giving the stability to the protein-inhibitor and protein-protein complexes.

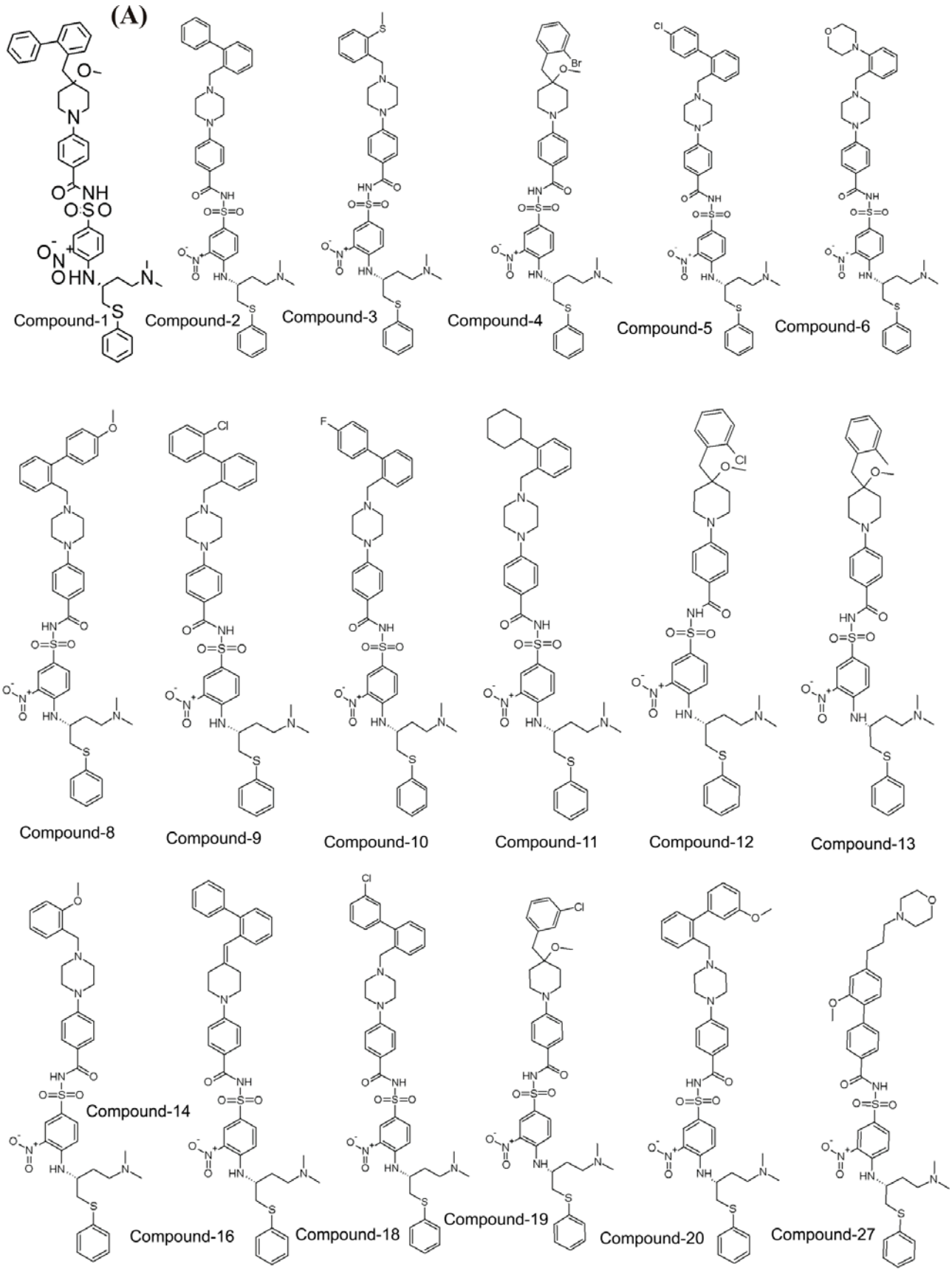
(A)
Compound-1
Compound-2
Compound-3
Compound-4
Compound-5
Compound-6
Compound-8
Compound-9
Compound-10
Compound-11
Compound-12
Compound-13
Compound-14
Compound-16
Compound-18
Compound-19
Compound-20
Compound-27

(B)

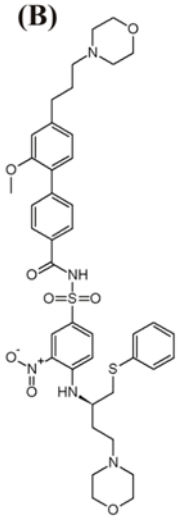

Compound-28

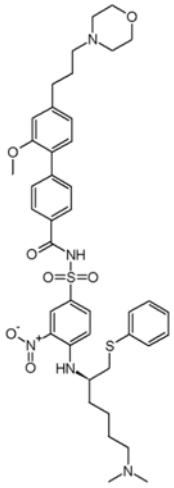

Compound-29

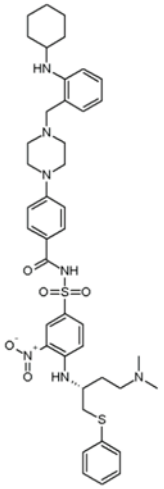

Compound-30

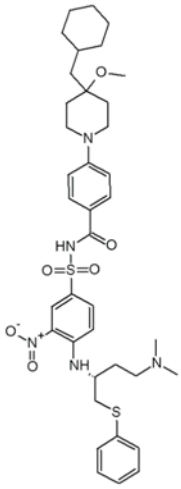

Compound-32

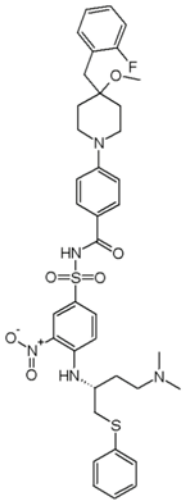

Compound-36

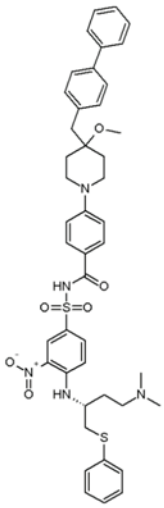

Compound-37

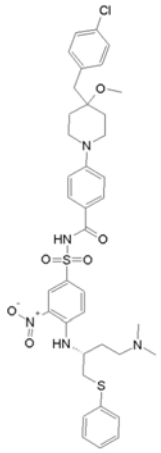

Compound-39

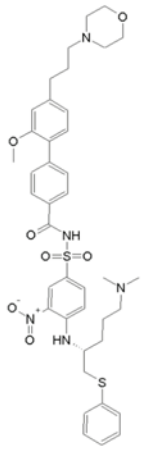

Compound-40

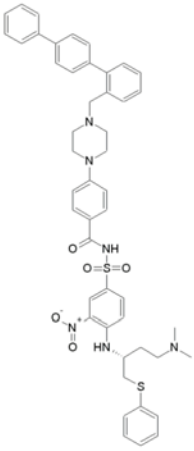

Compound-41

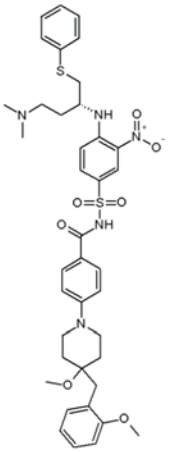

Compound-44

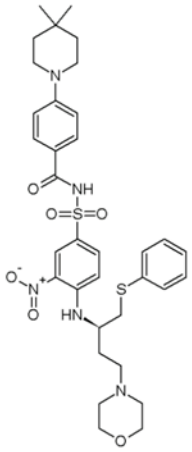

Compound-45

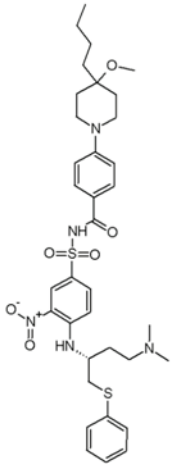

Compound-47

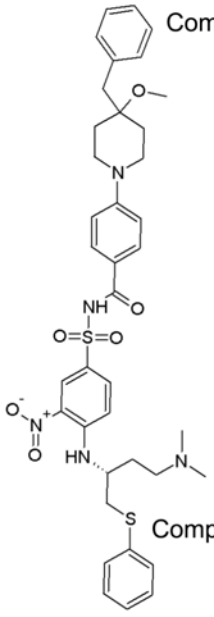

Compound-52

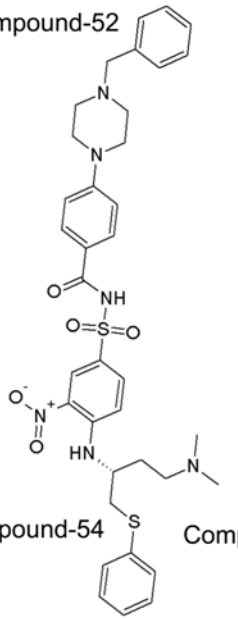

Compound-54

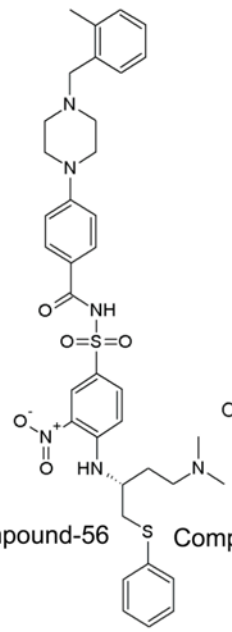

Compound-56

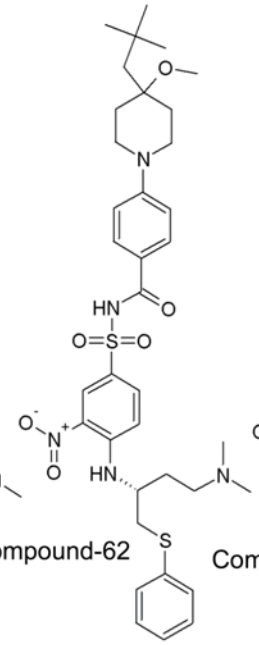

Compound-62

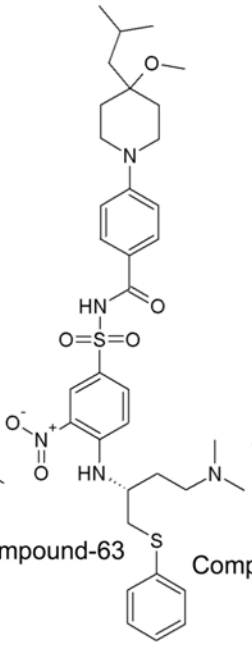

Compound-63

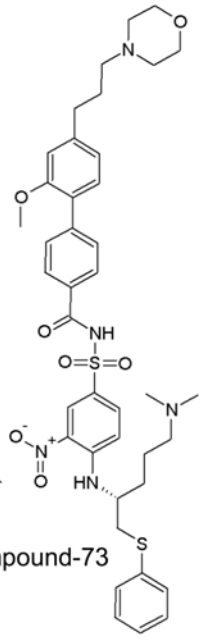

Compound-73

(C)

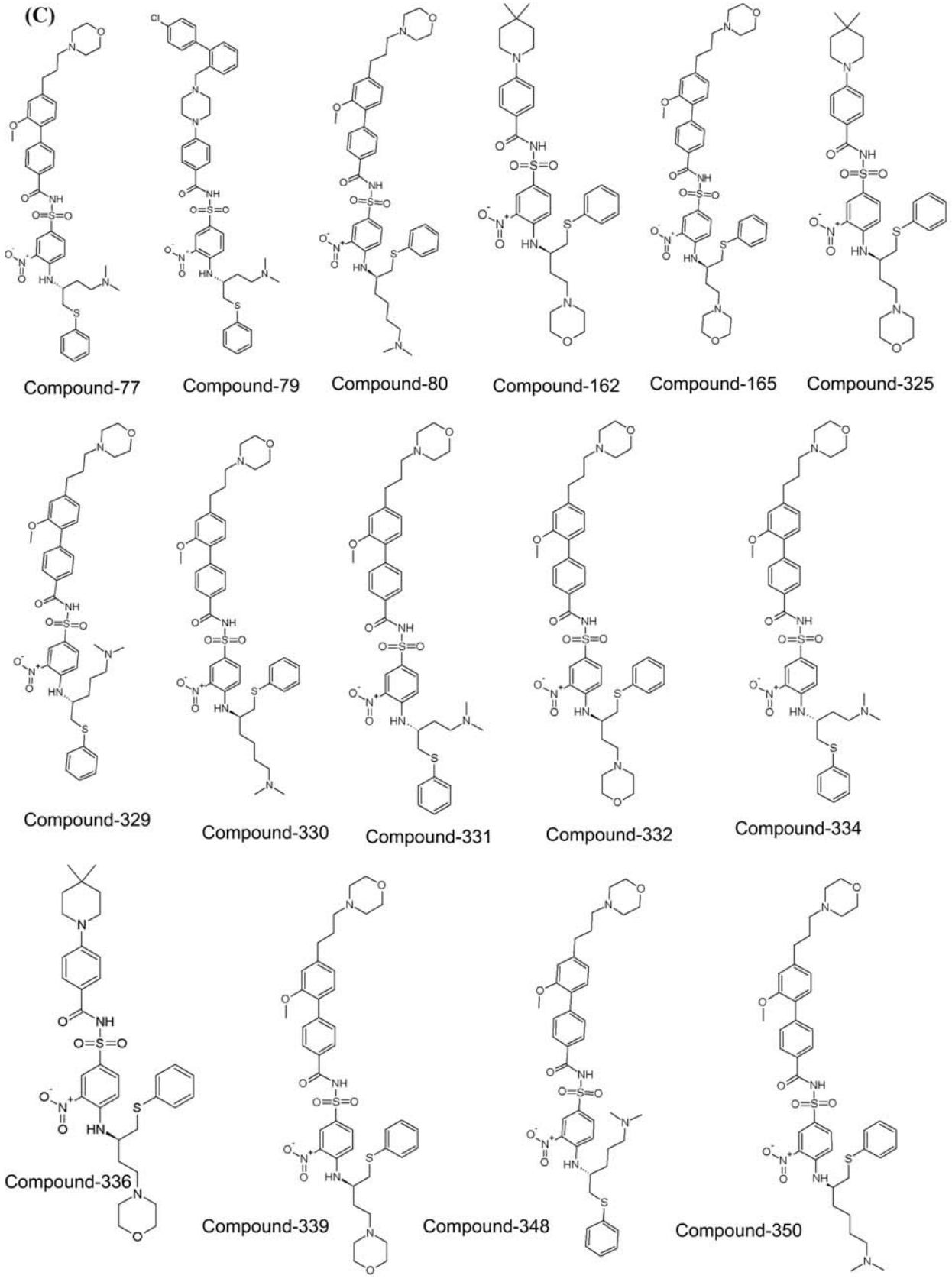
Compound-77
Compound-79
Compound-80
Compound-162
Compound-165
Compound-325
Compound-329
Compound-330
Compound-331
Compound-332
Compound-334
Compound-336
Compound-339
Compound-348
Compound-350

(D)

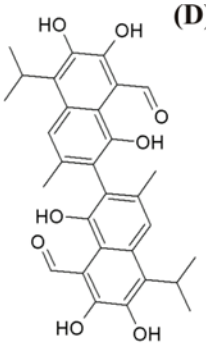

Compound-90

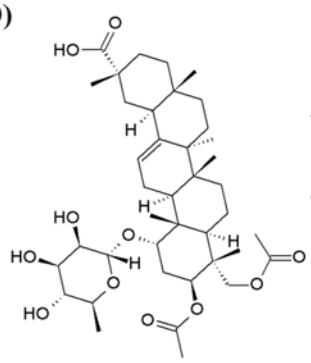

Compound-150

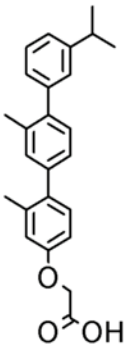

Compound-167

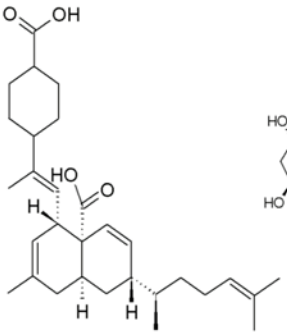

Compound-168

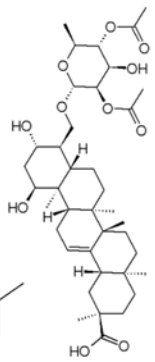

Compound-177

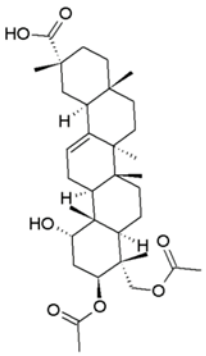

Compound-178

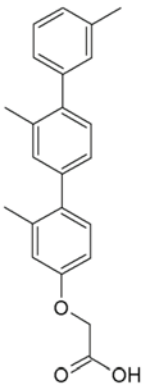

Compound-179

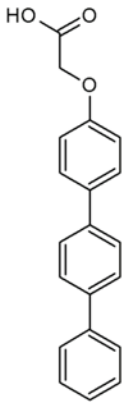

Compound-188

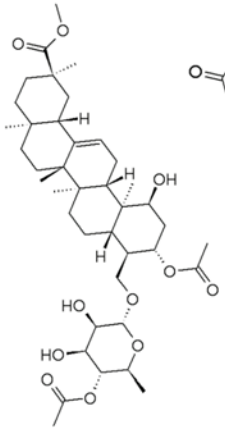

Compound-199

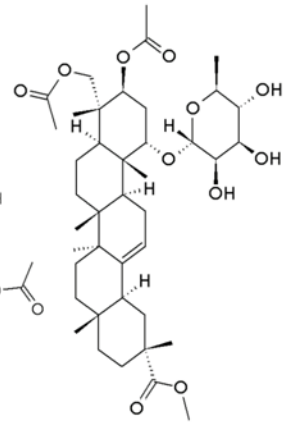

Compound-200

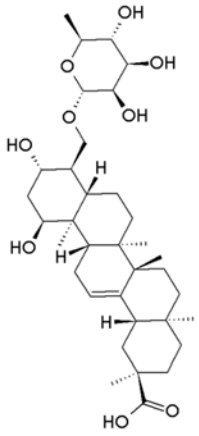

Compound-201

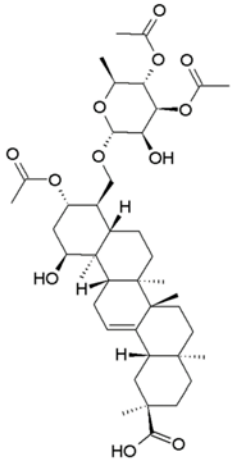

Compound-202

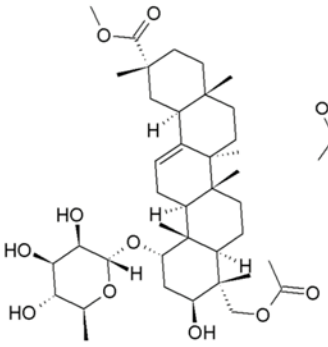

Compound-203

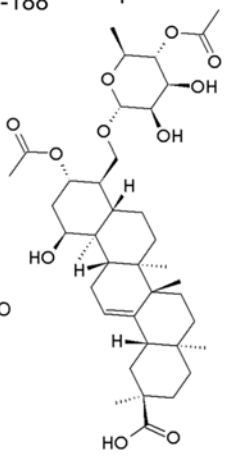

Compound-205

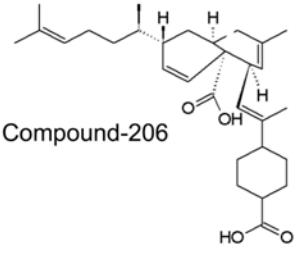

Compound-206

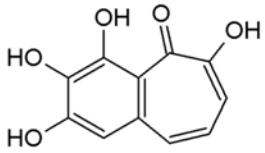

Compound-236

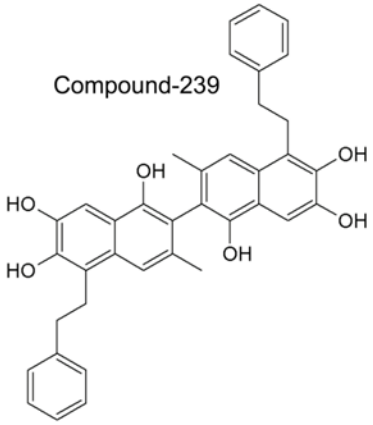

Compound-239

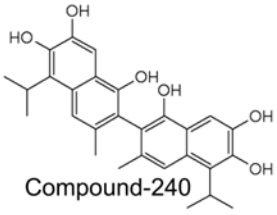

Compound-240

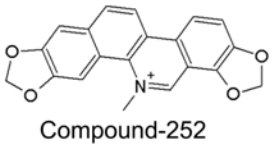

Compound-252

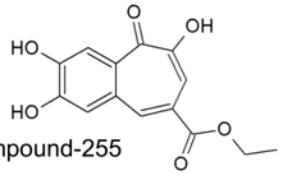

Compound-255

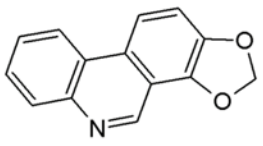

Compound-256

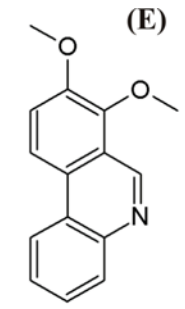

Compound-263

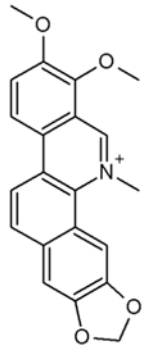

Compound-265

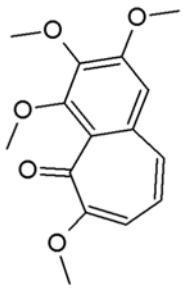

Compound-266

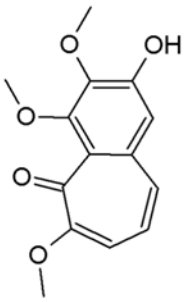

Compound-267

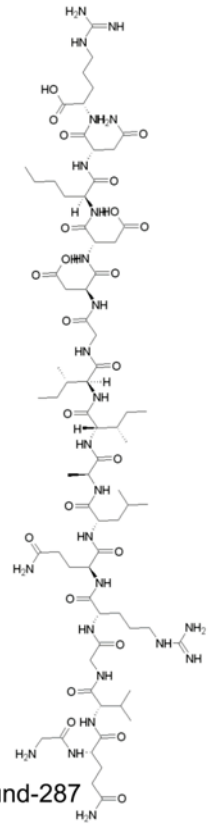

Compound-287

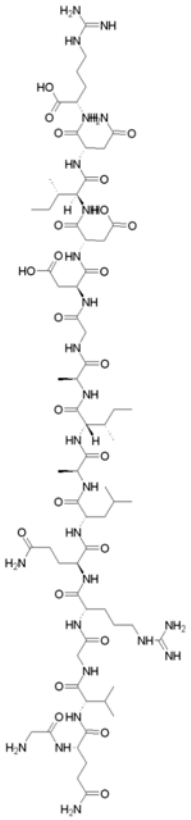

Compound-288

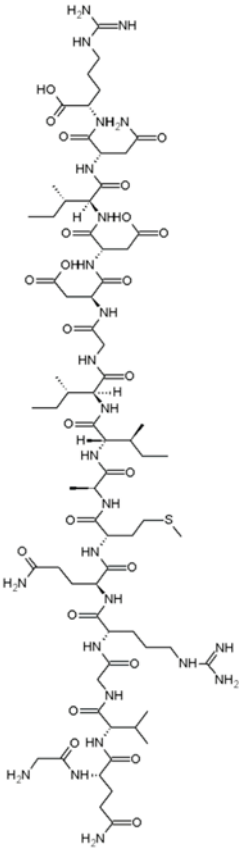

Compound-280

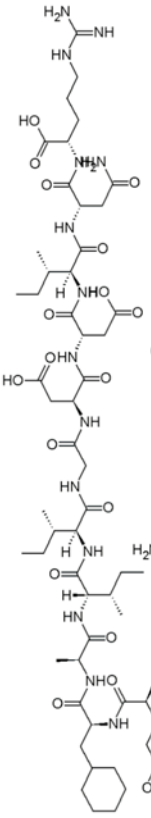

Compound-283

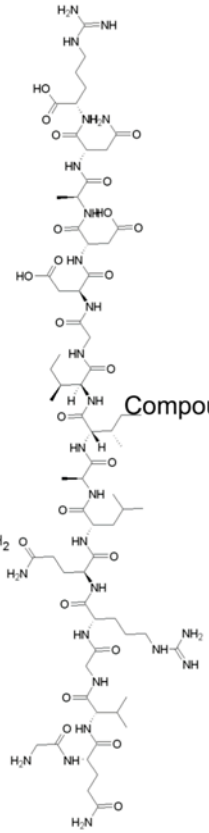

Compound-284

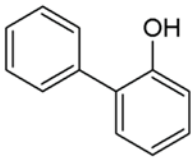

Compound-299

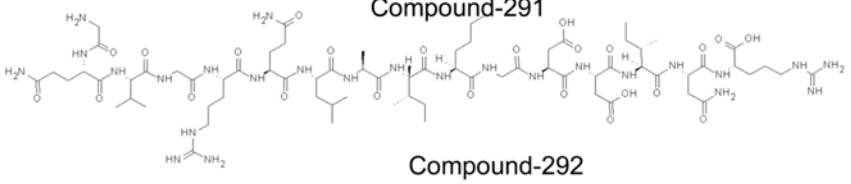

Compound-291

Compound-292

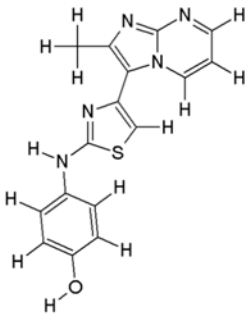

Compound-310

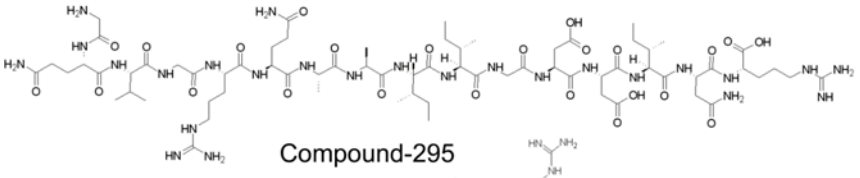

Compound-295

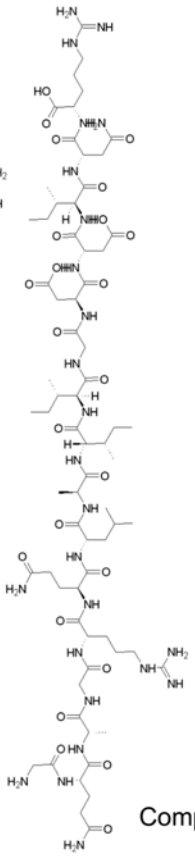

Compound-296

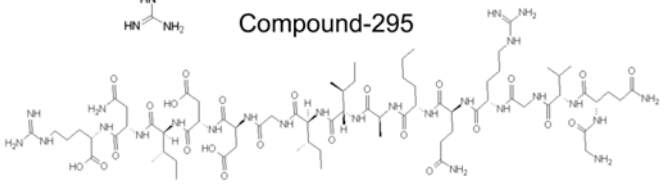

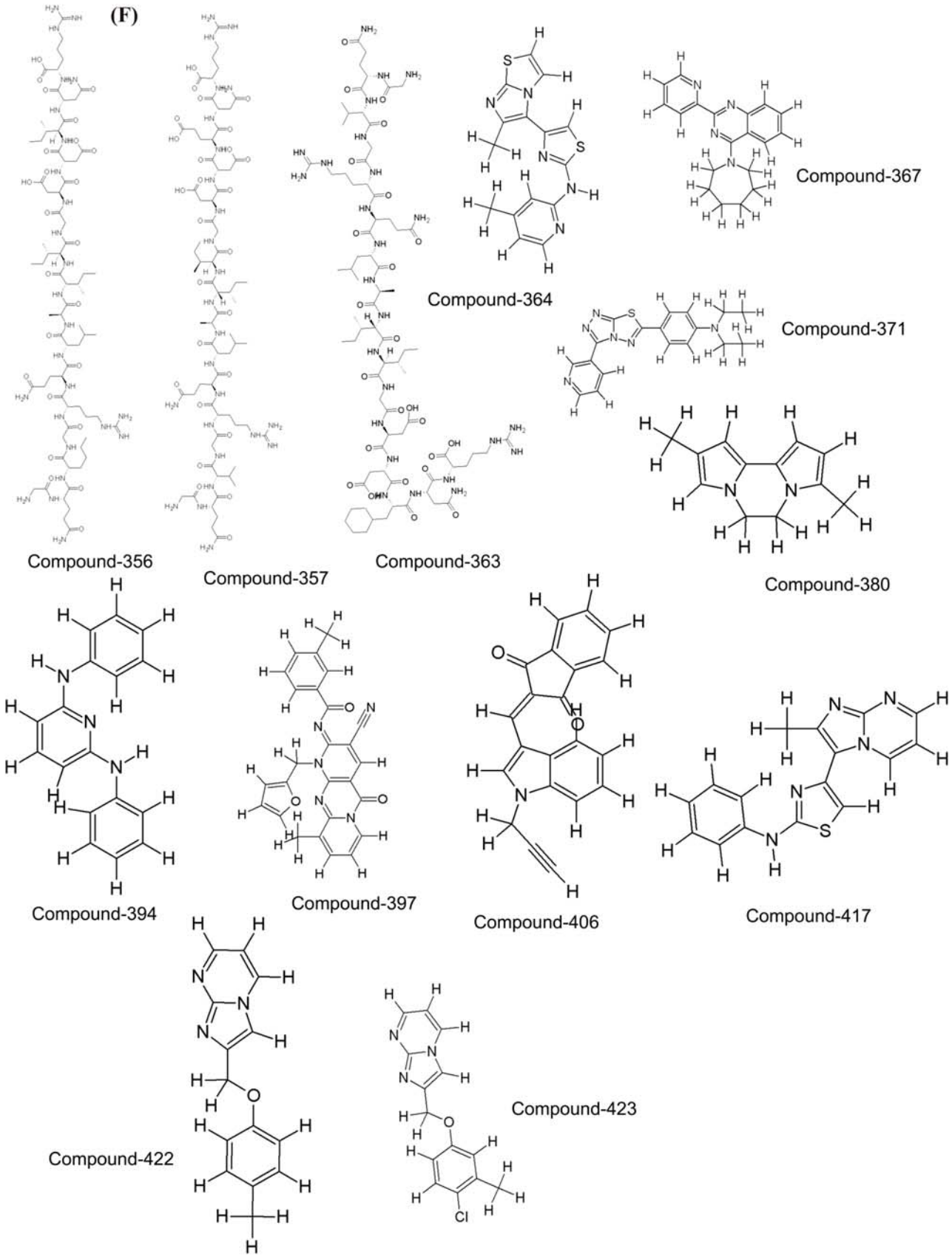

Figure 1. Inhibitors used for docking studies

Chemical structure of 51 higher similarity group (A, B, C) and 49 lower similarity group (D, E, F) inhibitors dataset used for the inhibition of apoptosis.

Table 2. Calculated Energies and RMSD for Protein Complexes with high Similarity group Potential Inhibitors

Compound No.	E[b]	V_{dw}-H_b-D_s	I[c]	T[d]	BE[e]	Ki (nM)	RMSD	IC_{50} (nM)	ΔG
1	+0.80	-10.10	-1.92	+3.57	-7.65	2460	0.150	<60.0	-7.74921
2	+0.42	-11.58	-1.50	+3.02	-9.64	86.24	0.165	<60.0	-9.75968
3	+0.25	-10.58	-1.76	+3.84	-8.25	891.97	0.077	<60.0	-8.3579
4	+0.10	-9.40	-3.74	+3.29	-9.75	71.84	0.156	<60.0	-9.86929
5	-0.05	-10.69	-1.84	+3.02	-9.56	97.54	0.139	<60.0	-9.6858
6	+0.17	-11.63	-1.54	+3.02	-9.99	47.71	0.143	<60.0	-10.1149
8	+0.07	-9.95	-1.74	+3.29	-8.33	783.7	0.206	<60.0	-8.43554
9	-0.06	-8.27	-2.26	+3.02	-7.57	2820	0.179	<60.0	-7.66726
10	-2.01	-7.49	-1.46	+3.02	-7.94	1520	0.228	<60.0	-8.03808
11	-1.28	-10.65	-1.81	+3.02	-10.72	13.92	0.152	61	-10.854
12	-1.69	-9.27	-2.25	+3.29	-9.93	53.03	0.170	62	-10.0514
13	-1.55	-8.13	-2.71	+3.29	-9.10	214.2	0.192	71	-9.21381
14	-1.52	-7.02	-3.16	+3.84	-7.86	1720	0.228	80	-7.96391
16	+0.52	-11.22	-1.96	+3.84	-8.82	341.18	0.116	83	-8.93451
18	+0.14	-10.30	-2.11	+3.02	-9.25	165.09	0.171	140	-9.37007
19	-0.52	-9.61	-0.98	+3.29	-7.82	1870	0.128	170	-7.91374
20	+0.17	-10.76	-1.66	+3.29	-8.95	272.9	0.164	178	-9.0685
27	-0.06	-9.98	-2.71	+4.94	-7.82	1860	0.098	n/a	-7.91696
28	-0.20	-11.01	-2.22	+4.94	-8.49	600.48	0.147	n/a	-8.59532
29	-0.07	-9.72	-2.91	+5.49	-7.21	5210	0.149	n/a	-7.29896
30	-0.69	-7.64	-2.65	+3.29	-7.69	2310	0.244	370	-7.78696
32	-0.49	-9.29	-1.35	+3.29	-7.84	1790	0.101	300	-7.93998
36	+0.80	-10.22	-2.03	+3.29	-8.16	1050	0.065	79	-8.26003
37	-0.31	-10.20	-2.28	+3.57	-9.22	174.83	0.171	160	-9.33567
39	-0.70	-10.31	-1.50	+3.29	-9.22	175.24	0.117	200	-9.33427
40	-0.62	-10.04	-2.35	+5.21	-7.80	1910	0.130	n/a	-7.90104
41	-0.70	-8.48	-3.61	+3.29	-9.49	110.09	0.309	100	-9.61318
44	+0.74	-11.52	-1.75	+3.57	-8.95	273.87	0.106	75	-9.06637
45	-0.53	-10.13	-1.60	+3.57	-8.69	423.16	0.085	n/a	-8.80531
47	+0.09	-11.21	-1.84	+4.12	-8.85	327.71	0.029	312	-8.95868
52	+0.14	-10.22	-1.60	+3.29	-8.39	709.13	0.117	150	-8.49554
54	+0.04	-9.81	-1.58	+3.57	-7.78	1980	0.068	n/a	-7.87945
56	+0.38	-11.26	-1.17	+3.02	-9.03	239.51	0.058	140	-9.1468
62	+0.43	-10.48	-1.60	+3.84	-7.81	1890	0.035	440	-7.90736
63	-0.94	-9.81	-1.38	+3.84	-8.28	850.01	0.065	360	-8.38681
73	-0.73	-8.39	-2.51	+5.21	-6.42	19690	0.150	n/a	-6.50124

(Table 2) Contd….

Compound No.	E^b	V_{dw}-H_b-D_s	I^c	T^d	BE^e	Ki (nM)	RMSD		IC_{50} (nM)	ΔG
77	-0.21	-8.81	-3.34		+4.94	-7.42	3650	0.127	n/a	-7.51247
79	-0.12	-9.37	-1.75		+3.02	-8.21	958.48	0.194	n/a	-8.31475
80	-0.59	-6.91	-4.08		+5.49	-6.09	34620	0.213	n/a	-6.16265
162	-0.63	-9.92	-1.99		+3.57	-8.98	262.97	0.099	n/a	-9.09074
165	-0.00	-8.15	-2.78		+4.94	-5.99	40760	0.180	n/a	-6.06469
325	-0.05	-9.35	-2.51		+3.57	-8.34	766.93	0.075	n/a	-8.44852
329	-0.66	-7.32	-3.54		+5.21	-6.31	23760	0.120	n/a	-6.3885
330	-0.65	-7.93	-3.03		+5.49	-6.11	32960	0.182	n/a	-6.19213
331	-0.51	-9.63	-2.44		+4.94	-7.64	2510	0.124	n/a	-7.73714
332	-0.07	-9.07	-2.23		+4.94	-6.43	19490	0.168	n/a	-6.50737
334	-0.65	-8.80	-3.00		+4.94	-7.51	3140	0.159	n/a	-7.60277
336	-0.55	-9.54	-1.88		+3.57	-8.40	692.84	0.066	n/a	-8.50948
339	-0.26	-9.89	-2.61		+4.94	-7.82	1840	0.144	n/a	-7.92345
348	-0.95	-7.35	-3.12		+5.21	-6.20	28390	0.278	n/a	-6.28168
350	-0.14	-8.71	-2.89		+5.49	-6.25	26270	0.173	n/a	-6.32825

E^b	The electrostatic component of binding free energy in kcal/mol.
V_{dw}-H_b-D_s	Van der waals, Hydrogen bond-Desolvation energy component of binding free energy in kcal/mol.
I^c	Total internal energy of binding in kcal/mol.
T^d	Torsional energy of binding in kcal/mol.
BE^e	Estimated binding free energy in kcal/mol.
RMSD	Root mean square deviation
ΔG	Gibbs free energy in kcal/mol.
Ki	Inhibitory constant in nanomolar (nM).
IC_{50}	Inhibitory concentration in nanomolar (nM).

However, in the dissimilar group the compound-150 and compound-205 have optimal energies and exhibits only hydrogen bond interactions with the protein, therefore they are not considered as the best inhibitors in this group. Complex formed by the compounds-177, 199, 200 and 239 considered as less stable as they form good interactions with the binding pocket regardless of their poor docking score. Compound-201 is selected as the best inhibitor due to optimal docking score and good interactions. This protein-inhibitor complex is stabilized by one salt bridge (Glu96:Arg100), one pi-pi interaction with Phe97, four hydrogen bonds with Ala93, Phe97, Tyr101 as well as with Gly138 residues of the binding pocket. Rest of the compounds in the lowest and highest similarity group were screened out due to either fewer interactions or the lower docking scores. The earlier reported compound considered as the reference compound [20] has lower energy than the selected inhibitors and their interactions are also poor with the protein in comparison to the new inhibitors identified in this study [20]. It forms only one hydrogen bond interaction with protein binding pocket *via* Glu129. The best inhibitors are broadly classified into two groups namely; 4 alkyl-4-methoxypiperidine derivative 8h where R= 4-Cl-Ph (including piperidine scaffold) and pentacyclic triterpenoid derivative compound-201 (including terpenoid scaffold). Compound-39, compound-1 (reference compound) is showing 1.117Å and 0.150Å root mean square deviation from the potent inhibitor compound-201.

Models for Inhibitors (potent) Binding and their Affinity

On the basis of the analysis, we predicted that the compound-201 i.e. pentacyclic triterpenoid derivative (analogue of oleanolic acid) inhibitor, would bind to Phe97of Bcl-xl *via* CD2 in pi-pi interaction and with Ala93 *via* O, Phe97 *via* N, Tyr101 *via* OH and Gly138 *via* O by hydrogen bond, respectively and there is one additional salt bridge between Glu96:Arg100, present in the binding pocket of the protein which provides the stability to the binding pose given in

Table 3. Calculated Energies and RMSD for Protein Complexes with Low Similarity Group Potential Inhibitors

Compound No.	E[b]	V_{dw}-H_b-D_s	I[c]	T[d]	BE[e]	Ki (nM)	RMSD	IC_{50} (nM)	ΔG
90	-0.04	-6.97	-0.52	+1.10	-6.43	19330	0.232	n/a	-6.51231
150	+0.09	-10.81	-0.27	+0.82	-10.16	35.52	0.110	n/a	-10.2919
167	-0.26	-7.28	-0.73	+1.65	-6.62	14040	0.177	n/a	-6.70416
168	-0.38	-8.63	-0.96	+2.20	-7.78	2000	0.098	n/a	-7.87342
177	-0.30	-9.14	-0.98	+1.92	-8.50	590.14	0.214	n/a	-8.60574
178	-0.01	-8.78	-0.40	+1.92	-7.27	4730	0.135	n/a	-7.35695
179	-0.77	-5.81	-0.70	+1.37	-5.91	46370	0.182	n/a	-5.98731
188	-0.65	-6.40	-0.53	+1.37	-6.21	27900	0.238	n/a	-6.29213
199	-0.06	-8.74	-1.02	+1.65	-8.18	1020	0.173	n/a	-8.27742
200	-0.03	-9.81	-0.49	+1.92	-8.40	691.56	0.162	n/a	-8.51059
201	+0.03	-10.28	-0.34	+1.37	-9.23	172.62	0.000	>100000	-9.3433
202	-0.05	-7.95	-1.42	+2.47	-6.95	8020	0.235	n/a	-7.04014
203	-0.32	-8.22	-0.07	+1.10	-7.52	3070	0.230	n/a	-7.6163
205	+0.01	-10.78	-0.53	+1.92	-9.38	132.8	0.116	n/a	-9.50065
206	-0.22	-8.61	-0.75	+2.20	-7.39	3840	0.124	n/a	-7.48202
236	+0.01	-5.94	+0.00	+0.00	-5.93	44860	0.327	2200	-6.00718
239	-0.11	-8.55	-1.08	+1.65	-8.10	1160	0.075	3500	-8.20025
240	+0.05	-6.96	-0.44	+0.55	-6.80	10330	0.138	3700	-6.88827
252	-0.01	-6.02	+0.00	+0.00	-6.03	38000	0.225	19000	-6.10675
255	+0.06	-6.76	-0.24	+0.82	-6.12	32460	0.352	73000	-6.2013
256	+0.00	-5.45	+0.00	+0.00	-5.45	101020	0.304	>100000	-5.52012
263	-0.03	-5.71	-0.07	+0.55	-5.25	141070	0.306	>100000	-5.31975
265	+0.03	-5.98	+0.00	+0.00	-5.95	43480	0.210	100000	-6.02593
266	-0.33	-5.19	-0.45	+1.10	-4.87	268850	0.241	>100000	-4.93281
267	-0.11	-5.36	-0.14	+0.82	-4.78	315380	0.275	>100000	-4.83704
280	+1.56e+07	+1.56e+07	+0.00	+15.09	+3.12e+07	-	0.975	n/a	-
283	+1.65	+19.51	+253.59	+13.99	+288.74	-	1.177	n/a	-
284	+1.56e+07	+1.59e+07	+0.00	+13.45	+3.15e+07	-	0.424	n/a	-
287	+1.56e+07	+1.60e+07	+0.00	+14.27	+3.16e+07	-	0.398	n/a	-
288	+1.56e+07	+1.57e+07	+0.00	+14.27	+3.12e+07	-	0.398	n/a	-
291	+1.54e+07	+1.59e+07	+0.00	+14.27	+3.13e+07	-	0.425	n/a	-
292	+1.55e+07	+1.61e+07	+0.00	+14.27	+3.16e+07	-	0.388	n/a	-
295	+1.54e+07	+1.59e+07	+0.00	+14.54	+3.13e+07	-	0.419	n/a	-
296	+1.48e+07	+1.52e+07	+0.00	+13.72	+2.99e+07	-	0.354	n/a	-
299	-0.03	-5.42	-0.21	+0.27	-5.39	111620	0.346	n/a	-5.46025
310	-0.27	-6.89	-0.78	+1.10	-6.84	9680	0.299	n/a	-6.92727

(Table 3) Contd….

Compound No.	E^b	V_{dw}-H_b-D_s	I^c	T^d	BE^e	Ki (nM)	RMSD	IC_{50} (nM)	ΔG
356	+1.56e+07	+1.59e+07	+0.00	+15.37	+3.15e+07	-	0.419	n/a	-
357	+1.53e+07	+1.61e+07	+0.00	+15.09	+3.14e+07	-	0.359	n/a	-
363	+1.58e+07	+1.63e+07	+0.00	+13.99	+3.22e+07	-	0.399	n/a	-
364	+0.00	-6.78	-0.28	+0.82	-6.24	26520	0.296	n/a	-6.32257
367	-0.03	-6.63	-0.41	+1.37	-5.70	66000	0.198	n/a	-5.77551
371	-0.06	-6.50	-0.36	+0.55	-6.38	21150	0.233	n/a	-6.45832
380	-0.04	-4.61	+0.00	+0.00	-4.65	389020	0.339	n/a	-4.71113
394	+0.00	-6.49	-0.42	+1.10	-5.81	55130	0.246	n/a	-5.88349
397	+0.03	-7.64	-0.58	+1.10	-7.10	6210	0.130	n/a	-7.19361
406	+0.01	-7.58	-0.49	+0.82	-7.24	4950	0.246	n/a	-7.32967
417	-0.86	-6.17	-0.46	+0.82	-6.67	12950	0.250	n/a	-6.75265
422	-0.70	-5.85	-0.23	+0.82	-5.96	42800	0.312	n/a	-6.03538
423	-0.77	-6.00	-0.30	+0.82	-6.24	26550	0.302	n/a	-6.32189

* Abbreviations as in the above table.

Fig. (**2A**). Arg100, Arg103, Arg139 are the key residues which form the "arginine fingers", the highly conserved residues. The highest similarity compound-39 i.e. 4-alkyl-4-methoxypiperidine derivative 8h (where R= 4-Cl-Ph)would bind to Arg139 and Ala142 through hydrogen as well as pi-pi interactions *via* NE and NE2 of Arg139, O of Ala142, S of Tyr101 and a salt bridge is formed within Arg103:Asp107 residues of the binding pocket as shown in Fig. (**2B**). There is also a conserved "arginine finger" formed by Arg139 and Arg103 which plays an important role to induce the apoptosis. This compound displayed strong pan-active inhibitory properties against Bcl-xL. The inhibitory constant Ki for protein–inhibitor binding was calculated which exhibits a strong correlation with the binding energy. Lower Ki values directly relate to the docking energy and inversely to the binding affinity that is the inhibitor having the lower inhibitory constant shows the higher affinity to the protein [20].

Compound-201 and compound-39, the potent inhibitors of Bcl-xL has the absolute free energy of binding, -9.3433 and -9.33427 kcal/mol whereas binding energies are -9.23 and -9.22 kcal/mol, respectively. An inverse relation was observed between Gibbs energy and binding energy for the formation of the protein-inhibitor complex similar to the Ki (inhibitor constant) and ΔG [23]. The Ki of the compound-201, 39 are 172.62nM and 175.24nM, respectively. These results indicate that there is a good correlation between the binding free energy and the biological activity [24]. The relation between computational derived inhibition constant (Ki) correlates well with the experimental Ki values of the compounds, derived from the database (http://www.bindingdb.org/) Fig. (**3**). This correlation may be helpful for further structure-based design of potent inhibitors.

DISCUSSION

The present study identifies the new potent inhibitors pentacyclic triterpenoid derivative (2S,4aR,6aR,6bS,8aS, 10R,12R,12aS,12bR,14bR,E)-10,12-dihydroxy-2,4a,14b-trimethyl-9-((((R)-3,4,5-trihydroxy-6-methyl-2H-pyran-2-yl) oxy)methylene)-1,2,3,4,4a,5,6,6a,6b,8a,9,10,11, 12,12a,12b, 13,14b-octadecahydropicene-2-carboxylic acid, and 4-alkyl-4-methoxypiperidine derivative 8h (where R= 4-Cl-Ph) distinct from the earlier known biarylacylsulfonamide antagonists for inhibiting the anti-apoptotic effect of the Bcl-xL protein. These new inhibitors are more potent in terms of its specificity and binding affinity. Furthermore, the specific interaction of potent inhibitor with the hydrophobic binding pocket was established and cross validated using results from the Sybyl Software package. The neighboring hydrogen bonds and salt bridges provide additional stability to the complex interactions giving necessary specificity to orient the helices of the protein [25, 26]. Earlier studies have shown that the anti-apoptotic protein Bcl-xL is known to maintain cell survival through the regulation of ion and metabolite gradients that enhance the sensitivity of ion channel activity [5]. The long A chain comprising of 197 residues of anti-apoptotic Bcl-xL protein is used in the present study for studying the protein-inhibitor interactions. The protein is established as an important drug target owing to its proposed role in regulating cell survival [28].

The protein is crucial for an array of apoptosis programmes, including developmentally programmed cell death, tissue turnover and host defense against pathogens [28]. The structure of the Bcl-xL protein consists of seven amphipathic α-helices joined by flexible loops. The hydrophobic interactions play a prominent role in the expulsion of water from the membrane contributing towards the stability of the protein-inhibitor complex [29].

In this study, the structural information of the protein from previous studies [5] was exploited for docking various compounds, in the quest for identifying new anti-apoptotic inhibitors exhibiting more potential than existing ones. The

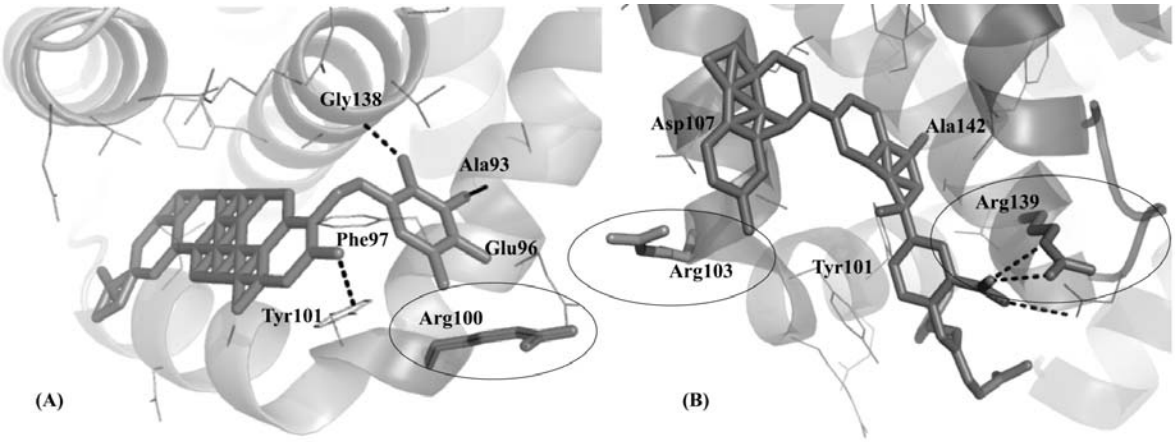

Figure 2. Cartoon representation of Compound-201 and compound-39 showing interaction in the binding pocket.
Cartoon representation of Compound-201 and compound-39 showing interaction in the binding pocket.
(**A**) Compound-201 forms hydrogen bonding with Ala93, Phe97, Tyr101 and Gly138. Residues Glu96 and Arg100 forms the salt bridge where as Phe97 is involved in both hydrogen bond and pi-pi stacking. (**B**) Compound-39 shows hydrogen bonding with Arg139 and Ala142 whereas Tyr101 and Asp107, Arg103 are involved in pi-pi and salt bridge interactions, respectively. Residues Arg100 and Arg139 comprising the "Arginine Finger" is shown as stick.

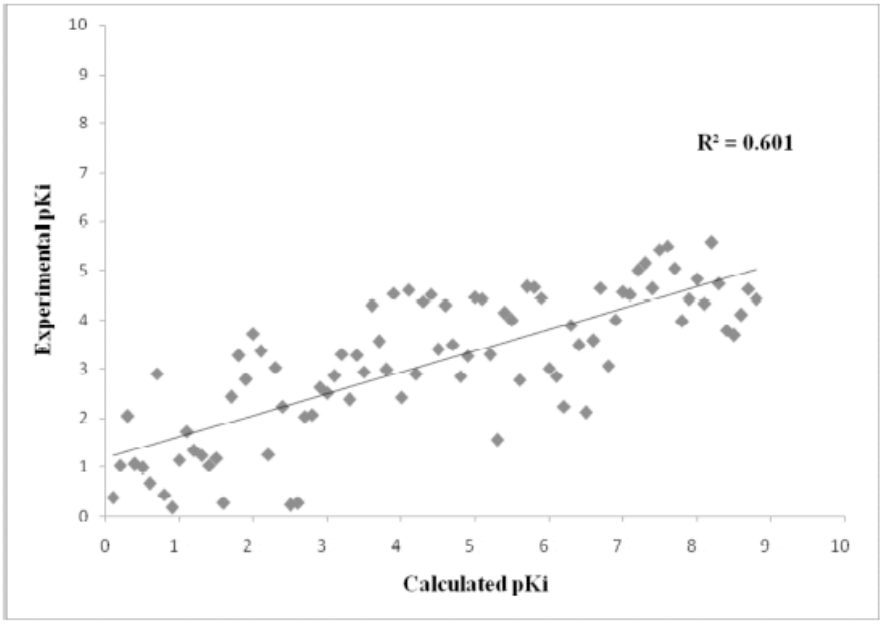

Figure 3. Correlation of the computational studies with the experimental determination of inhibition constants.

new compounds exhibit interactions that are stabilized by multitude of interactive forces. The geometry of face–to-face salt bridge and cation-pi interactions between conserved amino acids and protein-inhibitor provide more stability to the complex [30, 31]. Consequently, all of these interactions play potential role in increasing the affinity of the protein pocket for the inhibitor. Furthermore, the arrangement and nature of the amino acids in the binding pocket are important for the determination of the extent of interactions between the protein and the inhibitors. Arg, Asp, Phe, Ala, Tyr, Gly and Glu are the major residues that contribute towards the protein-inhibitor complex interactions. Ala93, Tyr101, Gly138 are only involved in the hydrogen bond interactions where as Phe97 forms both hydrogen bond and pi-pi interactions. The Glu96 and Arg100 are also involved in salt bridge formation in compound-201. Similarly, Arg139 and Ala142 forms hydrogen bond interactions where as Tyr101 is involved in pi-pi interactions. The Arg103 and Asp107 are also involved in salt bridge formation on interaction with compound-39.

The highly conserved arginine finger residues are observed in the binding pocket. It is shown to act by displacing water out of the binding niche that enhances the catalysis of electrostatic field [32, 33]. In other words, ''arginine finger'' pushes out the protein-bound structured water molecules. In the present study Arg100, Arg103 and Arg139 residues are the conserved arginine residues that are proposed to catalyze

the reaction by pushing out the water molecules. An inverse relation was observed between Gibbs energy / binding energy as well as Ki and ΔG of the protein-inhibitor complex. The results indicated a good correlation between the binding free energy and the biological activity. IC_{50} is concentration of inhibitor that is necessary for 50% inhibition of the effect of the disease. It was observed that increase in the LogP value supports the inhibitory activity of the IC_{50} of the molecules [34]. LogP is a key parameter to study the environmental fate of chemicals, used as a measure of molecular hydrophobicity which ultimately affects the drug absorption, bioavailability, hydrophobic drug-receptor interactions, metabolism of molecules, as well as their toxicity [34]. Ki values obtained from the docking results correlates well with the experimentally derived IC50 values from the binding database. Therefore our results are related to the experimental outcome, however our methodology includes only in silico experiments (Fig. **3**). In the light of these facts, we can include the correlation between docking values and experimental IC50 values. The correlation between these parameters is helpful for further structure-based design of potent inhibitors. The results further suggest that the increased binding affinity of the molecule favored overall interactions with surrounding residues in the binding pocket and the inhibitors having the lower inhibitory constant show higher affinity for protein.

In summary, we contend that the compounds pentacyclic triterpenoid derivative (2S,4aR,6aR,6bS,8aS,10R,12R, 12aS,12bR,14bR,E)-10,12-dihydroxy-2,4a,14b-trimethyl-9-((((R)-3,4,5-trihydroxy-6-methyl-2H-pyran-2-yl)oxy)methylene)-1,2,3,4,4a,5,6,6a,6b,8a,9,10,11, 12,12a,12b,13,14b-octadecahydropicene-2-carboxylic acid and 4-alkyl-4-methoxypiperidine derivative 8h (where R= 4-Cl-Ph) serve as inhibitor for anti-apoptotic Bcl-xL protein. The aspects of the anti-apoptotic protein must indeed be considered, because compound-201, 39 inhibitors bind to anti-apoptotic Bcl-xL protein. The new findings are shaping our impressions on both possibilities and challenges for anticancer drug design. Drugs based on the small molecules docking and finger printing studied here might be useful against HNSCC that over-express Bcl-xL proteins. The usefulness of the predicted compound for anticancer drug development will eventually be determined by their abilities to decrease Bcl-xL expressions in living cells and to selectively target cancerous versus healthy cells.

ABBREVIATIONS

Bcl-xL = B-cell lymphoma-extra large protein

HNSCC = head and neck squamous cell carcinoma

DISCLOSURE STATEMENT

No competing financial interests exist.

ACKNOWLEDGEMENT

The support of Department of Biotechnology, Ministry of Science and Technology, Government of India, to Bioinformatics Centre at Biotech Park Lucknow is gratefully acknowledged. We would like to thank Department of Radiotherapy and Chemotherapy, Chhatrapati Shahuji Maharaj Medical University, Lucknow, U. P. India for useful discussions during the course of this work.

SUPPLEMENTARY MATERIAL

Supplementary material is available on the publishers Web site along with the published article.

REFERENCES

[1] Thatte, U.; Dahanukar, S. Apoptosis: clinical relevance and pharmacological manipulation. *Drugs*, **1997**, *54*, 511-32.

[2] Billen, L.P.; Kokoski, C.L.; Lovell, J.F.; Leber, B.; Andrews, D.W. Bcl-XL inhibits membrane permeabilization by competing with Bax. *PLoS Biol.*, **2008,** *6*, e147. doi: 10.1371/journal.pbio.0060147

[3] Vijayalingam, S.; Subramanian, T.; Ryerse, J.; Varvares, M.; Chinnadurai, G. Down-regulation of multiple cell survival proteins in head and neck cancer cells by an apoptogenic mutant of adenovirus type 5. *Virology*, **2009**, *392*, 62-72.

[4] Fennell, D.A.; Corbo, M.V.; Dean, N.M.; Monia, B.P.; Cotter, F.E. *In vivo* suppression of Bcl-XL expression facilitates chemotherapy-induced leukaemia cell death in a SCID/NOD-Hu model. *Br J Haematol*. **2001**, *112*, 706-13.

[5] Priyadarshi, A.; Roy, A.; Kim, K.S.; Kim, E.E.; Hwangm, K.Y. Structural insights into mouse anti-apoptotic Bcl-xl reveal affinity for Beclin 1 and gossypol. *Biochem Biophys Res Commun.*, **2010,** *394*, 515-21.

[6] Lee, E.F.; Czabotar, P.E.; Smith, B.J; Deshayes, K.; Zobel, K.; Colman, P.M.; Fairlie, W.D. Crystal structure of ABT-737 complexed with Bcl-xL: implications for selectivity of antagonists of the Bcl-2 family. *Cell Death Differ*., **2007,** *14*, 1711-3.

[7] Bruncko, M.; Oostm, T.K.; Belli, B.A.; Ding, H.; Joseph, M.K.; Kunzer, A.; Martineau, D.; McClellan, W.J.; Mitten, M.; Ng, S.C.; Nimmer, P.M.; Oltersdorf, T.; Park, C.M.; Petros, A.M.; Shoemaker, A.R.; Song, X.; Wang, X.; Wendt, M.D.; Zhang, H.; Fesik, S.W.; Rosenberg, S.H.; Elmore, S.W. Studies leading to potent, dual inhibitors of Bcl-2 and Bcl-xL. *J Med Chem.*, **2007**, *50*, 641-62.

[8] Berman, H.M.; Westbrook, J.; Feng, Z.; Gilliland, G.; Bhat, T.N.; Weissig, H.; Shindyalov, I.N.; Bourne, P.E. The Protein Data Bank. *Nucleic Acids Res.*, **2000,** *28*, 235-42.

[9] Morris, G.M.; Goodsell, D.S.; Halliday, R.S.; Huey, R.; Hart, W.E.; Belew, R.K.; Olson, A.J. Automated docking using a Lamarckian genetic algorithm and an empirical binding free energy function. *J Comput Chem.*, **1998**, *19*, 1639-62.

[10] Bikadi, Z.; Hazai, E. Application of the PM6 semi-empirical method to modeling proteins enhances docking accuracy of AutoDock. *Journal of Cheminformatics*, **2009,** *1*, 15. doi: 10.1186/1758-2946-1-15.

[11] Labute, P. Protonate 3D: Assignment of Macromolecular Protonation State and Geometry. Chemical Computing Group Inc **2007**.

[12] Morris, G.M.; Huey, R.; Lindstrom, W.; Sanner, M.F.; Belew, R.K.; Goodsell, D.S.; Olson, A.J. AutoDock4 and AutoDockTools4: Automated docking with selective receptor flexibility. *J Comput Chem.*, **2009**, *30*, 2785-91.

[13] Lee, M.S.; Olson, M.A. Calculation of absolute ligand binding free energy to a ribosome-targeting protein as a function of solvent model. *J Phys Chem B.*, **2008**, *112*, 13411-7.

[14] Shaikh, S.A.; Ahmed, S.R.; Jayaram, B. A molecular thermodynamic view of DNA-drug interactions: a case study of 25 minor-groove binders. *Arch Biochem Biophys.*, **2004**, *429*, 81-99.

[15] Jenwitheesuk, E.; Samudrala, R. Improved prediction of HIV-1 protease-inhibitor binding energies by molecular dynamics simulations. *BMC Struct Biol*., **2003**, *3*, 2. doi:10.1186/1472-6807-3-2.

[16] Yoshikawa, T,; Tsukamoto, K.; Hourai, Y.; Fukui, K. Improving the accuracy of an affinity prediction method by using statistics on shape complementarity between proteins. *J Cjem Inf Model*., **2009,** *49*, 693-703.

[17] Sikic, M.; Tomic, S.; Vlahovicek, K. prediction of protein-protein interaction sites in sequences and 3D structures by random forests. *Plos Comput Biol.*, **2009**, 4:e1000278.

[18] Wei, J.; Rega, M.F.; Kitada, S.; Yuan, H.; Zhai, D.; Risbood, P.; Seltzman, H.H.; Twine, C.E.; Reed, J.C.; Pellecchia, M. Synthesis and evaluation of Apogossypol atropisomers as potential Bcl-xL antagonists. *Cancer Lett.*, **2009,** *273*, 107-13.

[19] Wei, J.; Kitada, S.; Rega, M.F.; Stebbins, J.L.; Zhai, D.; Cellitti, J.; Yuan, H.; Emdadi, A.; Dahl, R.; Zhang, Z.; Yang, L.; Reed, J.C.; Pellecchia, M. Apogossypol derivatives as pan-active inhibitors of antiapoptotic B-cell lymphoma/leukemia-2 (Bcl-2) family proteins. *J Med Chem.*, **2009,** *52*, 4511-23.

[20] Wei, J.; Kitada, S.; Rega, M.F.; Emdadi, A.; Yuan, H.; Cellitti, J.; Stebbins, J.L.; Zhai, D.; Sun, J.; Yang, L.; Dahl, R.; Zhang, Z.; Wu, B.; Wang, S.; Reed, T.A.; Wang, H.G.; Lawrence, N.; Sebti, S.; Reed, J.C.; Pellecchia, M. Apogossypol derivatives as antagonists of antiapoptotic Bcl-2 family proteins. *Mol Cancer Ther.*, **2009,** *8*, 904-13.

[21] Pena, J.C.; Thompson, C.B.; Recant, W.; Vokes, E.E.; Rudin, C.M. Bcl-xL and Bcl-2 expression in squamous cell carcinoma of the head and neck. *Cancer.* **1999**, *85*, 164-70.

[22] Dunkel, M.; Gunther, S.; Ahmed, J.; Wittigm B.; Preissner, R. SuperPred: drug classification and target prediction. *Nucleic Acids Res.*, **2008**, *36*, W55-9.

[23] Tian, G.; Haffnerm C.D. Linear Relationships between the Ligand Binding Energy and the Activation Energy of Time-dependent Inhibition of Steroid 5α-Reductase by Δ1-4-Azasteroids. *Journal of Biological Chemistry*. **2001,** *276*, 21359-64.

[24] Ali, H.I.; Fujita, T,; Akaho, E.; Nagamatsu, T. A comparative study of AutoDock and PMF scoring performances, and SAR of 2-substituted pyrazolotriazolopyrimidines and 4-substituted pyrazolopyrimidines as potent xanthine oxidase inhibitors. *J Comput Aided Mol Des.*, **2010,** *24*, 57-75.

[25] Gupta, S.; Misra, G.; Pant, M.C.; Seth, P.K. Prediction of a new surface binding pocket and evaluation of inhibitors against huntingtin interacting protein 14: an insight using docking studies. *J Mol Model.*, **2011**, *17*, 3047–56.

Received: February 16, 2012 **Revised: March 30, 2012** **Accepted: April 11, 2012**

[26] Gupta, S.; Misra, G.; Pant, M.C.; Seth, P.K. Targeting the epidermal growth factor receptor: exploring the potential of novel inhibitor N-(3-Ethynylphenyl)-6, 7-bis (2-methoxyethoxy) quinolin-4-amine using docking and molecular dynamics simulation. *Protein Pept Lett.*, **2012**.

[27] Misra, G,; Aggarwal, A.; Dube, D.; Zamanm M.S.; Singh, Y.; Ramachandran, R. Crystal structure of the acillus anthracis nucleoside diphosphate kinase and its characterization reveals an enzyme adapted to perform under stress conditions. *Proteins.*, **2009**, *76*, 496-506.

[28] Youle, R.J.; Strasser, A. The BCL-2 protein family: opposing activities that mediate cell death. *Nat Rev Mol Cell Biol.*, **2008**, *9*,47-59.

[29] Pace, C.N.; Shirley, B.A.; McNutt, M. Gajiwala, K. Forces contributing to the conformational stability of proteins. *FASEB J.*, **1996**, *10*, 75-83.

[30] Dougherty, D.A. Cation-pi interactions involving aromatic amino acids. *J Nutr.*, **2007,** *137*, 1504S-8S; discussion 16S-17S.

[31] Pecsi, I.; Leveles, I.; Harmat, V.; Vertessy, B.G.; Toth, J. Aromatic stacking between nucleobase and enzyme promotes phosphate ester hydrolysis in dUTPase. *Nucleic Acids Res.*, **2010**, *38*, 7179-86.

[32] te Heesen, H.; Gerwert, K.; Schlitter, J. Role of the arginine finger in Ras.RasGAP revealed by QM/MM calculations. *FEBS Lett.*, **2007,** *581*, 5677-84.

[33] Kotting, C.; Kallenbach, A.; Suveyzdis, Y.; Wittinghofer, A.; Gerwert, K. The GAP arginine finger movement into the catalytic site of Ras increases the activation entropy. *Proc Natl Acad Sci U S A.*, **2008**, *105*, 6260-5.

[34] Latha, P.P.D.; Sharmila, J.S.D. QSAR study for the prediction of IC50 and Log P for 5-N-Acetyl-Beta-DNeuraminic Acid structurally similar compounds using stepwise (multivariate) linear regression. *International Journal of Chemical Research.* **2010**, *2*, 32-8.

View publication stats